Rapid, simple and sustainable synthesis of ultra-microporous carbons with high performance for CO_2 uptake, via microwave heating

Gabriela Durán-Jiménez[*1], Lee A. Stevens[1], Emily T. Kostas[2], Virginia Hernández-Montoya[3], John P. Robinson[1], Eleanor R. Binner[1]

[1]Faculty of Engineering, the University of Nottingham, University Park, Nottingham, NG7 2RD, U.K.

[2] Department of Biochemical Engineering, The Advanced Centre of Biochemical Engineering, Bernard Katz Building, University College London, Gower Street, London, WC1H 6BT, U.K.

[3]TecNM/Instituto Tecnológico de Aguascalientes, Av. Adolfo López Mateos No. 1801 Ote. C.P. 20256, Aguascalientes, México.

* Corresponding author

e-mail: gaby_231105@yahoo.com.mx/gabriela.duranjimenez@nottingham.ac.uk

Tel: +44 (0)77 2793 4248

Abstract

A one step microwave pyrolysis-activation method has been developed for the preparation of activated carbons from biomass with high CO_2 capture efficiency (5.3 mmol g^{-1}) by employing a low impregnation ratio (1) of KOH and K_2CO_3. The high microwave susceptibility identified by the dielectric properties enabled the preparation of a series of activated carbons in short processing times (<6 min), and the pyrolysis-activation simultaneously enhanced the formation of ultra-micropores leading to high CO_2 uptake at 15 and 100% CO_2 in the temperature range of 0-100 °C. The high CO_2/N_2 selectivity of up to 36 the adsorptive capacities were directly correlated to a pore size of ~0.7 nm, which favoured CO_2 uptake up to 5.3 and 4.5 mmol g^{-1} at 1.1 bar and 0 °C and an uptake of 3.7 and 3.3 at 25 °C for activated samples with KOH and K_2CO_3, respectively. The activated carbons presented in this study are the first examples of samples that have been prepared by this simple and rapid method, which represents a 96.66% reduction in the processing times in comparison to conventional heating routes, and the CO_2 uptake is comparable to the largest reported in literature for activated carbons. The outstanding uptake and selectivity, the simple synthesis using microwave technology in addition to the utilisation of a waste biomass as a carbon precursor, satisfy the requirements for the development of new and more sustainable energy environmental processes.

KEYWORDS: CO_2 capture, Ultra-microporous adsorbents, Microwave, Selective uptake, Regeneration, Rapid sustainable preparation of activated carbons.

1 Introduction

It has been estimated that over two-thirds of the globally produced anthropogenic greenhouse gas emissions are generated by the burning of fossil fuels to produce energy [1]. From 1970 until 2004 the annual global emissions of Carbon Dioxide (CO_2) have increased by 80% [2] and the current air concentration (>400 ppm) exceeds the maximum permissible limit for climate safety (350 ppm) [3]. Consequently, an increase in global temperature from 1.8 to 4 °C is expected by the year 2100 as a result of global warming [4-6]. Although other greenhouse gases such as water vapour, methane (CH_4), and nitrous oxide (NO_x) contribute to global warming, 90% of the emissions are attributed to CO_2 [7]. In view of this, large-scale CO_2 control is essential to minimize the global impacts associated with climate change [8].

Cryogenic processes, membrane separation, chemical absorption and adsorption have been investigated for CO_2 capture and storage. In particular, chemical absorption with ammonia based absorbents (wet scrubbing) is currently being implemented on an industrial scale for CO_2 capture. This process commonly utilizes alkanolamine-functional groups such as monoethanol amine (MEA) which react with CO_2 from the flue gas in an absorber column. Despite the fact that absorption technologies can achieve efficiencies of up to 90%, there are several issues such as limited surface utilization, corrosion, volatilization/degradation and a significant energy penalty associated with material regeneration [9-11]. Due to the shortcomings of the conventional amine scrubbing process in CO_2 removal from flue gas, solid adsorption processes have been proposed as an alternative. In particular, gas adsorption on solids represents a well-developed technology used in many industries and offers several advantages for CO_2 capture applications compared to CO_2 absorption. These include no liquid wastes being produced and a wider temperature range application (25–700 °C) [12]. It has been found that porous materials have great potential as excellent inorganic solid adsorbents for CO_2 uptake

due to their high surface area and large pore volume. Zeolites, [13, 14] activated carbons, [15, 16] calcium and magnesium oxides, [17, 18] and metal organic frameworks, [15, 19] are some of the adsorbents extensively tested on the CO_2 capture. Activated carbon is one of the most utilized adsorbents due to its high surface area and chemical properties such as its hydrophobicity, which prevents an additional step for moisture removal prior to CO_2 adsorption. Furthermore, the 'green' credentials of activated carbons can be further enhanced if they are prepared from sustainable biomass resources that would normally be considered as waste residues [20].

To increase the CO_2 adsorption capacity of porous carbons, much attention has focussed on surface functionalisation with inorganic bases for the incorporation of basic sites, by generally preparing N-doped activated carbons. The carbon materials are treated with urea or NH_3 at high temperatures to incorporate N in the carbon matrix. Further activation of N-doped carbons is used to increase the surface area [21]. Traditionally, physical and chemical activation has been achieved using conventional furnaces. The physical activation consists of the gasification of a carbon precursor with oxidizing gases such as steam or air at high temperature (800-1100 °C). In the case of chemical activation, the precursor is first thermally treated (~700 °C) under inert conditions to obtain a carbon-rich material, which is later mixed with an activating agent such as H_3PO_4, $ZnCl_2$, KOH and K_2CO_3 and subsequently activated at high temperatures (800-1100 °C) [22, 23].

It has been found that the incorporation of N atoms in the carbon matrix coupled with chemical activation by KOH or K_2CO_3 results in a significant improvement in the adsorption of CO_2 [24]. Fujiki *et al*. [25] reported the enhanced CO_2 adsorption of chitosan derived activated carbon with N-doping and found the CO_2 adsorption to be 4.9 mmol g^{-1} at 1 bar and 25 °C. Zhang *et al*.[26] employed a NH_3 solution during carbonization to incorporate N-containing functional groups on the surface of synthesized activated carbons. A three-step procedure was

used where black locust biomass was first carbonized at 650 °C, then the resultant carbon was activated with a 6 times impregnation ratio of KOH:carbon at 830 °C, followed by modification with NH_3 solution at 600 °C. The CO_2 uptake at 25 °C was 5.5 mmol g^{-1} [26]. Although the aforementioned results are impressive, the preparation of N-doped carbons by functionalisation and an activation method requires high amounts of expensive and hazardous chemicals in a complex process, which may ultimately also damage the structure and properties of the porous carbon materials [27].

On the contrary, activated carbons using hydrochar as a precursor has also been reported. Sevilla *et al*. [28] demonstrated that by using an impregnation ratio of 2 (KOH/hydrochar), an activated carbon with a CO_2 uptake of 4.8 mmol/g was generated. However, the preparation of this carbon was relatively laborious as the synthesis of the hydrochar was firstly required, followed by an impregnation step and lastly the activation of the material. Furthermore, the high temperature step, undertaken by conventional heating is extremely energy intensive. Therefore, in order for activated carbons (for CO_2 capture) to become environmentally sustainable and economically viable, new manufacturing processes which utilise less energy and hazardous chemicals and fewer unit operations, are required.

In recent years, microwave heating has gained attention as a promising heating method, due to its characteristics of instantaneous and volumetric heating, which overcome the limitations of conventional heat transfer [29]. Microwave heating has been shown to offer significant benefits such as exceptionally rapid processing times and selectivity [30].

There are a few reports on single pyrolysis-activation of biomass via conventional heating, and the majority of the studies that do employ microwaves focused on the use of microwave heating for the activation stage of a carbon-rich material that has been pre-pyrolysed in conventional furnaces [31]. In the search for sustainable and more economically viable methods of activated

carbons preparation, it is desirable to simplify the synthesis process and in particular to negate the need for carbonisation prior to activation. In this paper, for first time a rapid method for the synthesis of ultra-microporous activated carbons in one step used for CO_2 capture is described. This route negates the requirement of high amount of activating agent (often 2:1 or even higher), the pre-carbonization step and also a significant reduction in processing times compared to the 4 – 6 h durations required in conventional processes, whilst delivering sustainable activated carbons with good properties for CO_2 capture. This represents a novel production route that could transfer the microwave preparation of activated carbons from laboratory novelty to industrial application, leading to significant reductions in capital and operating costs as well as environmental impact.

2 Experimental

2.1 Materials

Pecan nutshell (PNS) is a lignocellulosic agricultural co-product that was used as an activated carbon precursor in these studies. It was collected from an agro-food company in Aguascalientes, México. The composition of PNS was determined to be 47.27% C, 6.41% H, 0.18% N and 46.14% O. The activating agents used in this work, potassium hydroxide (KOH) and potassium carbonate (K_2CO_3) were of analytical grade and purchased from Sigma-Aldrich and used without any further purification.

The precursor was firstly crushed and sieved to obtain a particle size ~1 mm, washed with deionised water and dried in an oven at 80 °C for 24 h, then physically mixed with the chemical agent (i.e. KOH or K_2CO_3) at mass ratio 1:1 (KOH: PNS and K_2CO_3:PNS).

2.2 Dielectric properties measurements

The loss tangent ($\tan\delta = \varepsilon''/\varepsilon'$) is an estimation of the material's ability to convert electromagnetic energy into heat at a specific temperature and frequency. Dielectric properties

and the temperature dependence of impregnated PNS (KOH:PNS and K_2CO_3:PNS) were obtained using the cavity perturbation technique for a temperature range of 20–500 °C at 2450 MHz. The system consisted of a furnace and cylindrical TM_0n_0 mode cavity. An automated step-motor was used to rapidly move the sample from the furnace to the cavity, where the dielectric properties are measured by a HP 8753 vector network analyser (VNA).The sample was placed in a quartz tube of 3 mm (ID) and the dielectric properties were calculated using the cavity response between a load and empty tube. The results presented in this work are the averages of three replications.

2.3 In-situ Microwave Pyrolysis-Activation of biomass

The innovative direct pyrolysis-activation by microwave was conducted using a single mode cavity that operated at a frequency of 2450 ± 25 MHz and includes a generator with 2 kW maximum output power, an automatic three-stub tuner (S-TEAM STHD v1.5) connected to a rectangular WR430 waveguide and a sliding short. The automatic tuner and the sliding short were used for impedance matching, to maximise the absorbed power and to log the absorbed power over time so that an energy balance can be calculated. A cylindrical single mode TE_{010} cavity was connected by WR430 waveguide to the sliding short and the incident, absorbed and reflected powers were recorded. The pyrolysis-activation reactor consisted of a quartz tube (30 mm ID) with a sintered plate where the mixture (KOH:PNS or K_2CO_3:PNS) was placed. The mixture was pyrolysed-activated in a single step at incident powers of 300 and 400 W and times of 2 – 6 minutes (Table 1). The incident powers and treatment times were selected based on previously published work using the same single mode cavity [32]. All the experiments were carried out in an inert atmosphere of nitrogen (N_2) at a flow rate of 1 L min^{-1}. Once the target time was reached, the sample was maintained in the inert atmosphere for 5 min to cool down.

The surface temperature of the sample was measured with a thermocouple RS K-type 1319A immediately after each treatment. It should be noted that the temperature values are an indication of a single-point temperature reached by the sample surface during the pyrolysis-activation process, however a representative average temperature measurement is not possible due to the volumetric and instantaneous nature of the microwave heating process.

The percent of absorbed and reflected power was calculated from the signals of incident power, absorbed power and reflected power. The specific absorbed energy (E) was determined by numerical integration of the absorbed power, (P_a), according to the following equation:

$$E = \frac{\int P_a dt}{M} \quad (1)$$

Where E is the specific absorbed energy (kJ g^{-1}), t is time differential (sec), and M is the initial mass of the sample (g).

To calculate the yield, the final carbon was repeatedly washed with 0.1 M HCl and deionised water until a neutral pH was obtained and then dried at 105 °C overnight. It was found the yields ranged from 22 and 25% for both activated carbons prepared with KOH and K_2CO_3.

For convenience, the activated carbons were labelled as *x-y-KOH* and *x-y-K_2CO_3* where *x* is the incident power (W) and *y* is the pyrolysis-activation time (min).

Table 1. Processing conditions of activated carbons preparation in one step of pyrolysis-activation by microwave

Sample name	**Incident Power (W)**	**Time (min)**	**Absorbed energy (kJ/g)**	***Temperature (°C)**
300-3-KOH	300	3	4.52	312
300-4-KOH	300	4	6.35	392
300-5-KOH	300	5	8.07	405
300-6-KOH	300	6	11.32	451

400-2-KOH	400	2	4.28	353
400-3-KOH	400	3	6.36	422
400-4-KOH	400	4	6.74	446
300-3-K_2CO_3	300	3	6.45	224
300-4-K_2CO_3	300	4	8.16	296
300-5-K_2CO_3	300	5	10.67	305
300-6-K_2CO_3	300	6	13.49	375
400-2-K_2CO_3	400	2	4.26	263
400-3-K_2CO_3	400	3	5.20	292
400-4-K_2CO_3	400	4	6.93	283

*Measured with a thermocouple after microwave treatment

2.4 Characterisation techniques

The textural properties of the activated carbons were calculated from the sorption isotherms of N_2 at -196 °C using a Micromeritics ASAP 2420 apparatus from 0.00005 to 0.99 relative pressure (P/P_0). Approximately, 250 mg of samples was weighed into a sample tube and degassed for 15 h at 120 °C. The surface area was calculated using the Brunauer–Emmett–Teller (BET) theory, based on adsorption data in the range of 0.01–0.1 P/P_0 to give positive BET 'C' parameters. The narrow micropore, micropore and total pore volumes and size distributions were determined by Non-Local Density Functional Theory (NLDFT) on carbon slit pores by combining a CO_2 adsorption isotherm at 0 °C to a N_2 adsorption isotherm beginning at 0.0005 P/P_0 using Microactive Software V5.0.

XRD analysis was performed on a Bruker D8 Advance Da Vinci diffractometer, with 0.02 ° step size and step time of 10 sec in the 2θ range 10 - 80 °. The morphology of the samples was examined by Scanning Electron Microscopy (SEM) using a Philips XL 30 microscope.

Thermogravimetric analysis (TGA) was performed in alumina pans using a TA Instruments SDT Q600 analyzer. Samples were heated up to 950 °C at 15 °C min-1 under a flow of nitrogen at 25 ml min^{-1}.

2.5 CO_2 capture experiments

The CO_2 uptake was determined using volumetric and thermogravimetric analysers by a Micromeritics ASAP 2420 and TGA Q500 TA Instrument. The CO_2 uptake isotherms were obtained at 0 and 25 °C on a volumetric analyser. Prior the measurements the samples were degassed at 120 °C for 15 h. The adsorption capacity was investigated in terms of adsorbed amount (CO_2 99.99%) per gram in the pressure range of 0.001−1.2 bar.

The thermogravimetric CO_2 uptake was carried out using a Q500 TA instrument. The carbon samples were dried at 120 °C in N_2 (100 ml min^{-1}, 1 bar) for 30 min before being cooled to the set CO_2 adsorption temperature to remove any physiosorbed moisture. The CO_2 uptake was obtained at a variety of temperatures between 25 and 100 °C, at an atmospheric pressure of 1 bar. At adsorption temperature the gas was switched at 15% CO_2 and 100% CO_2. Once the adsorption reached equilibrium at a given temperature, the adsorbed amount of CO2 was recorded vs time for 60 min, then the sample was heated up to 120 °C in N_2 for 15 min to complete the CO_2 desorption. Cyclic adsorption and desorption tests were also conducted to study the stability and reusability of the samples. This procedure was repeated three times and the main of replications is presented.

The N_2 gas adsorption (for CO_2 and N_2 selectivity) was measured using a thermogravimetric analysis. Both set of experiments were conducted at 25 ° C. The sample was degassed under Ar at 120 °C and the gas was switched from Ar to N_2. The isosteric heat of adsorption (Q_{st}) was calculated using CO_2 adsorption isotherms measured at different temperatures based on the Clausius-Clapeyron equation:

$$ln\left(\frac{P_2}{P_1}\right) = \frac{Q_{st}}{R}\left(\frac{1}{T_1} - \frac{1}{T_2}\right) \quad (2)$$

where Pi is pressure for isotherm i; T_i is temperature for isotherm i; R is the universal gas constant 8.315 J $K^{-1}mol^{-1}$. In this study, the Q_{st} was calculated using CO_2 adsorption isotherms measured at 0 and 25 °C.

All experiments were conducted in triplicate and the data presented were obtained from the mean calculated. In general, standard deviations were below 5 % of average values.

3 Results and Discussion

3.1 Dielectric properties of impregnated PNS

Fig. 1 shows the loss factor, ε″, against temperature in the temperature range of 20 - 500 °C for the impregnated PNS samples, along with previously reported values for raw PNS measured using the same method [33]. Materials with ε″<0.01 require a very high electric field strength in order to attain a reasonable heating rate, whereas heating materials with ε″>5 may be problematic due to the low penetration depth causing non-uniformities of heating. Materials with loss factors within the range 0.01<ε″<5 are therefore considered to be good candidates for microwave heating applications [34].

The results in Fig. 1 show that the ε″ of the raw PNS is within the range 0.1 - 0.2 from 20-300 °C, but drops to close to the lower processing threshold (0.01) from 350 - 500 °C. Similar results have been reported previously for biomass such as switchgrass [35], rice husk [36], corn stover [37], oil palm shell [38], wood biomass [39], empty fruit bunch [40]. The findings highlighted biomass is low loss dielectric materials, and are essentially transparent to microwaves from room temperature to 500 °C. However, when the biomass samples are subjected to higher temperatures, the structures become essentially char, which is known to be a high microwave absorbing material due to the Maxwell–Wagner effect, which causes a very

high displacement of π-electrons on carbonized structures [41, 42]. Materials with $\varepsilon'' < 0.01$ require a very high electric field strength in order to attain a reasonable heating rate, whereas heating materials with $\varepsilon'' > 5$ may be problematic due to the low penetration depth causing non-uniformities of heating. Materials with loss factors within the range $0.01 < \varepsilon'' < 5$ are therefore considered to be good candidates for microwave heating applications [34].

The results in Fig. 1 show that the ε'' of the raw PNS is within the range 0.1 - 0.2 from 20-300 °C, but drops to close to the lower processing threshold (0.01) from 350 - 500 °C. Up to 200 °C, chemical impregnation of PNS with K_2CO_3 has little or no effect on the dielectric response; ε'' remains <0.2. The loss factor of PNS impregnated with KOH on the other hand increased from 0.5 at room temperature to 7.6 at 150 °C, and then reduced to 1.1 by 250 °C. This suggests that all three samples are adequate candidates for microwave heating up to 200 °C, however KOH:PNS is likely to heat more efficiently and this may be related to the moisture in the sample. From 250 to 450 °C, the ε'' of both of the impregnated samples stabilised around 0.3 - 1.2 (with KOH:PNS being slightly higher), which is higher than the virgin PNS. At 500 °C, ε'' increased to 1.0 and 1.8 for K_2CO_3 and KOH respectively, indicating that although the heating rate would increase if heated to 500 °C, thermal runaway should not be a problem if processing within this temperature range. The dielectric characterisation therefore indicates that both impregnated materials would be expected to heat with microwaves at temperatures of 250 °C and above, and that they should heat more readily than raw PNS within that range.

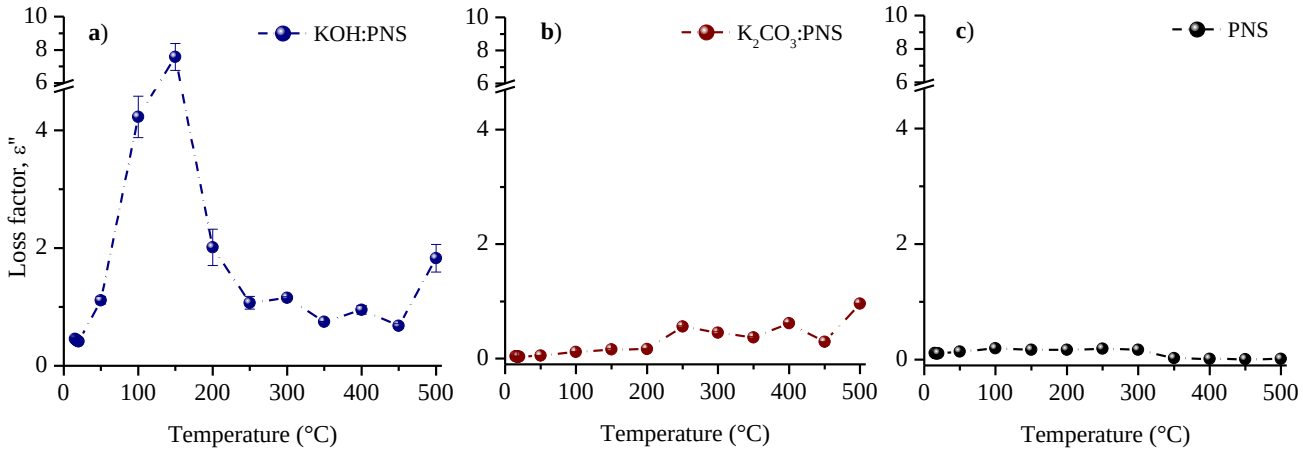

Fig. 1. Dielectric loss (ε′′) at 2450 MHz against temperature of (a) PNS:KOH, (b) PNS:K_2CO_3 and (c) PNS.

The impregnation of PNS with KOH and K_2CO_3 affected the dielectric loss of the material. Both impregnated materials have dielectric loss within the range that is considered amenable to microwave processing. Up to 250 °C, the dielectric loss of KOH:PNS is higher than K_2CO_3:PNS, suggesting good selectivity and heating rates during the microwave activation experiments.

3.2 Effect of processing time and micropore size of activated carbons

A significant amount of research has focussed on increasing the surface area of activated carbons, as it is generally assumed that higher surface areas and greater pore volumes generate more desirable absorbents for greater gas uptake [4]. The N_2 sorption isotherms and pore size distribution of the carbons prepared via single pyrolysis-activation at a mass ratio (KOH:PNS, K_2CO_3:PNS) of 1 are presented in Fig. 2 and the corresponding textural properties are summarized in Table 2. The two set of samples are generally similar, showing a type I-N_2 isotherm, according to the IUPAC classification, indicating the predominance of micropores in the activated carbons [43]. At lower pressures, there is evidence of a well-defined micropore filling stage, which suggests the presence of very small pores <1 nm which is corroborated in

the pore size distribution. The hysteresis loop shown in some samples suggest the presence of mesopores. The H4 loops are often found with aggregated crystals of zeolites, some mesoporous zeolites, and micro-mesoporous carbons [44].

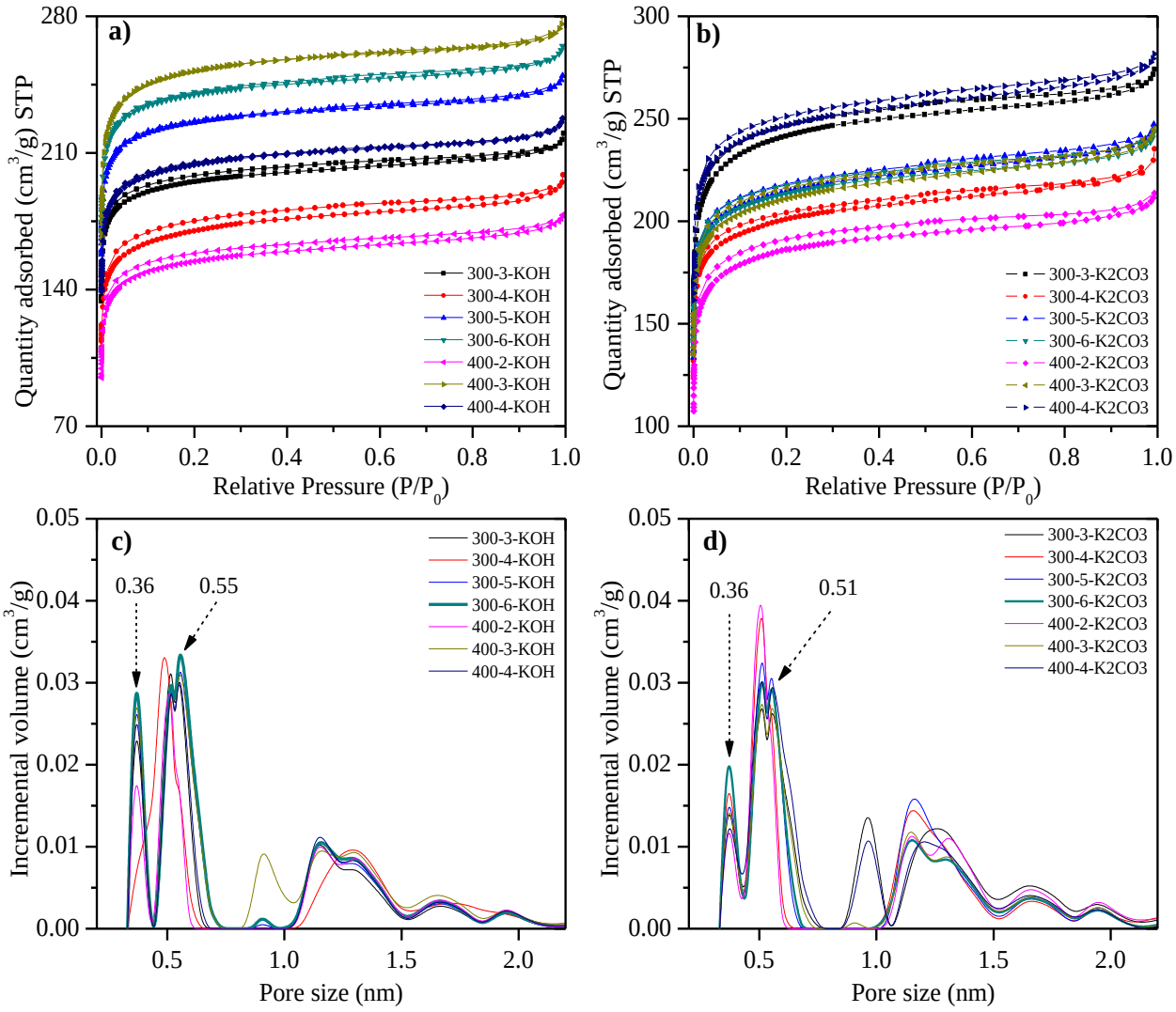

Fig. 2. N_2 adsorption-desorption isotherms at -196 (N_2) (a-b) and pore size distribution from combined N_2 (-196 °C) and CO_2 (0 °C) adsorption isotherms using NLDFT carbon slit model (c-d) of activated carbon prepared in single pyrolysis-activation by microwave

As summarized in Table 1 and 2, changing the power and time (energy) appeared to have an effect on the surface area and pore volume. The surface areas ranged from 608-1000 $m^2\ g^{-1}$ and 842-974 $m^2\ g^{-1}$ and pore volumes ranged from 0.25-0.39 $cm^3\ g^{-1}$ and 0.31-0.40 $cm^3\ g^{-1}$ for the

KOH and K_2CO_3 carbon samples, respectively. These results validate the applicability of a direct activation of biomass using low processing time with microwaves. Interestingly, Fig. S1 showed that in general the percent of pore volume ($V_{<0.8nm}$) for samples K_2CO_3 are comparable in the range of energies from 4.26 to 10.67 kJ g^{-1}, with a volume pore percent ($V_{<0.8nm}$) of 60.51 - 63.93%. However, for the KOH prepared samples, a more remarkable effect is presented which may be associated with the dielectric properties previously discussed. At an energy of 4.52 kJ g^{-1} the ($V_{<0.8nm}$) percent is 60.93% which increased up to 73.49% at 11.32 kJ g^{-1}. It should be noted, however, that 300-6-KOH possessed more abundant ultra-micropores (73.49 %) than the other carbons, as displayed in Fig. 2 and Table 2.

Despite the fact that the samples were prepared in rapid processing times (6 min), the activated carbons possessed a considerable micropore percent and surface area. In general, the surface area and pore volume of the activated carbons prepared in a single pyrolysis-activation are comparable or even higher to those of equivalent agent ratios prepared with more processing steps, by carbonisation followed by activation using conventional heating [45-47]. In certain cases, the surface area is also comparable to those prepared with higher amounts of agent: carbon ratio (i.e., 2:1 and 4:1) and conventional carbonisation and activation [48, 49]. This finding is of high importance, which confirms that the porosity is not compromised when microwave pyrolysis-activation is performed via the faster and more environmentally friendly processing route detailed in this work.

Table 2 Textural parameters of the series of activated carbons prepared in a single pyrolysis activation step using microwaves.

Sample	[a]S_{BET} (m^2/g)	[b]V_p (cm^3/g)	[c]$V_{<2nm}$ (cm^3/g)	[d]$V_{<0.8nm}$ (cm^3/g)	% ($V_{<0.8nm}$)
300-3-KOH	778	0.314	0.287	0.225	71.63
300-4-KOH	667	0.289	0.253	0.190	65.69
300-5-KOH	902	0.356	0.329	0.261	73.13
300-6-KOH	959	0.377	0.349	0.277	73.49
400-2-KOH	608	0.259	0.227	0.158	60.93
400-3-KOH	1000	0.394	0.365	0.260	66.13
400-4-KOH	811	0.327	0.296	0.228	69.92
300-3-K_2CO_3	947	0.389	0.346	0.226	58.22
300-4-K_2CO_3	789	0.334	0.294	0.209	62.53
300-5-K_2CO_3	844	0.357	0.312	0.224	62.83
300-6-K_2CO_3	842	0.351	0.310	0.234	66.89
400-2-K_2CO_3	728	0.312	0.275	0.189	60.51
400-3-K_2CO_3	827	0.351	0.303	0.222	63.31
400-4-K_2CO_3	974	0.401	0.354	0.257	63.93

[a] Specific surface area calculated by the BET method.
[b] Total pore volume recorded at 100 nm on cumulative pore volume by NLDFT carbon slit pore model.
[c] Micropore volume obtained at 2 nm on cumulative pore volume by NLDFT carbon slit pore model.
[d] Ultra-micropore volume obtained at 0.8 nm on cumulative pore volume by NLDFT carbon slit pore model

The development of larger pore sizes is due to gasification effects associated with the decomposition of potassium salts. The reaction between biomass carbon and KOH starts at low temperatures which leads to oxidation of carbon, resulting in the formation of K_2CO_3 and the hydroxide itself gets reduced to metallic potassium and hydrogen [50]. KOH dehydrates to

transform into K_2O at 400 °C, then the carbon is consumed by the reaction of carbon and H_2O with the emission of H_2. K_2CO_3 formed as a result of redox reactions can further react with biomass carbon to generate K_2O, metallic potassium and volatiles. Previous studies indicate K_2CO_3 is formed at about 400 °C and at 600 °C KOH is completely consumed. K_2CO_3 is decomposed into CO and K_2O at temperatures higher than 700 °C and disappears at temperatures around 800 °C [51].

$$Biomass + KOH \rightarrow Biomass.K_2O + H_2O(l)$$

$$Biomass + H_2O \rightarrow C + H_2O + tar$$

$$C + H_2O \rightarrow H_2 + CO$$

$$CO + H_2O \rightarrow H_2 + CO_2$$

$$2K_2O + H_2 + CO_2 + C \rightarrow C + 2K + H_2O + 2K_2CO_3$$

$$K_2CO_3 + C \rightarrow K_2O + 2CO$$

$$K_2O + C \rightarrow 2K + CO$$

Potassium metal (K) is produced during K_2O activation at high temperatures and it was found that the formation of pores was due to the loss of carbon (C). The activation involves the etching of the carbon framework via the redox reactions (listed above). The potassium vapour that is produced may penetrate between the carbon layers and induce swelling and disintegration of the carbon microstructure, thereby resulting in the framework expansion and generation of a porous network [4, 45, 46]. The potassium compounds formed during the process are subsequent removed using acid wash.

3.2.1 Morphology and chemical structure of activated carbons

Powder X-ray diffraction was used to analyse the nature of the inorganic species present in the materials after the microwave treatment and to corroborate the complete removal of K species after the washing. Fig. 3 shows the patterns of sample 300-6-KOH and 300-6-K_2CO_3,

respectively. It is observed that the only species remaining after the microwave pyrolysis-activation is the calcium carbonate ($CaCO_3$) in sample 300-6-KOH, which is confirmed in EDX (Fig. 3 c). The XRD pattern of the carbon materials are characteristic of activated carbons with amorphous structures showing broad and diffused peaks at 2θ= 30 °, which corresponds to the (002) set of planes related to the interlayer spacing, and at 43 ° (100), corresponding to the microcrystallinity

lateral dimension of (100) planes, respectively [46, 48, 52]. Sample 300-6-KOH additionally shows distinctive peaks for $CaCO_3$, which results from the transformation of the initial inorganic compound previously reported in the PNS biomass (calcium oxalate) [33].

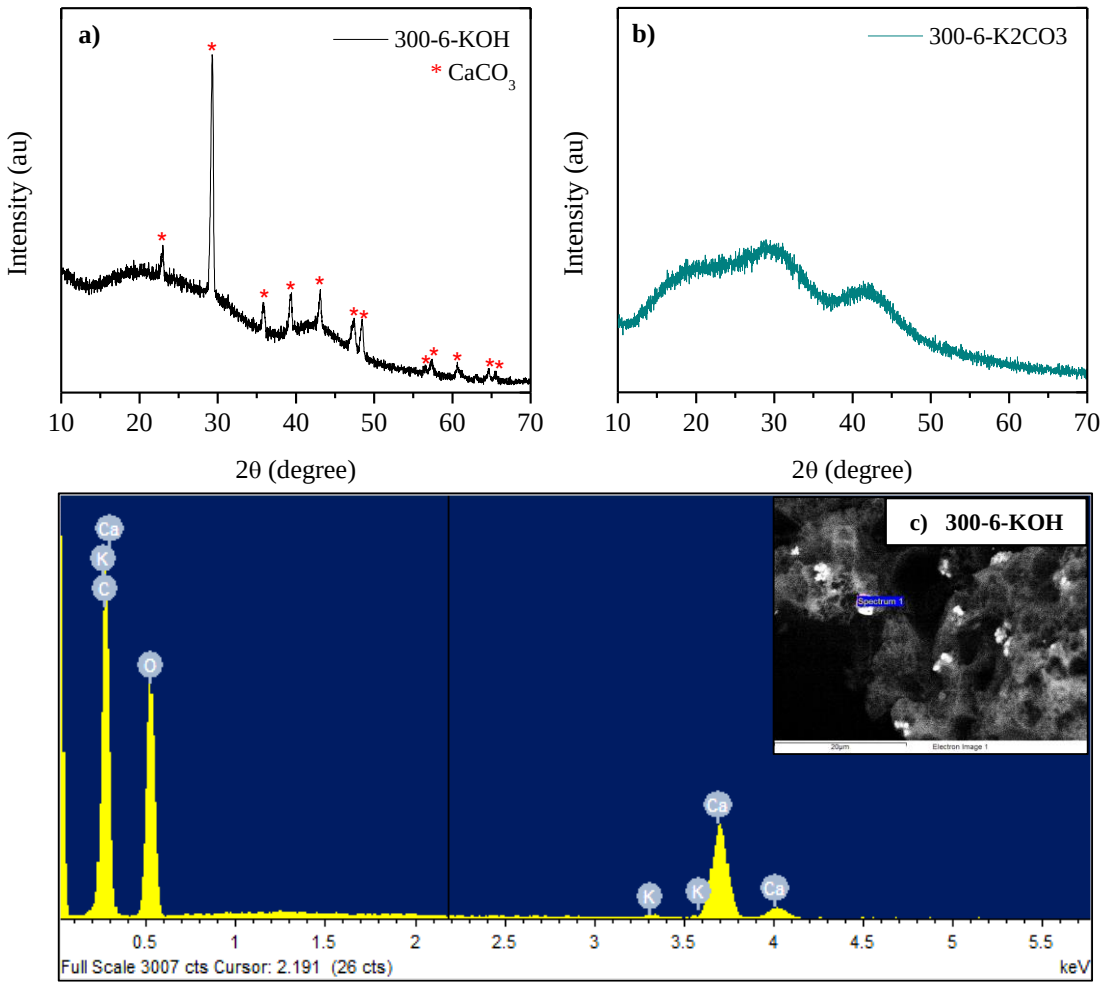

Fig. 3. XRD pattern of (a) 300-6-KOH and (b) 300-6-K_2CO_3 activated carbons, and (c) EDX analysis of 300-6-KOH carbon

The morphologies of the selected activated carbons prepared using KOH and K_2CO_3 were analysed by SEM, and the images are shown in Fig. 4. Additional morphologies of PNS biochar prepared at 300 W and 6 min without chemical impregnation is presented for comparison. Distinctive morphologies between char and activated carbons are illustrated. In both cases of activated carbons, the morphologies are dominated by particles with large conchoidal cavities, which are consistent with what has previously been reported for activated carbons. The morphology of KOH (Fig. 4 a, b) shows microsheets and possession of a large number of interconnected pores [53]. The SEM images of K_2CO_3 activated carbon (Fig. 4 c, d) show a material of irregular shapes and a rough topography. The SEM images indicate that the activated carbons are porous structures and the electron diffraction illustrates that the white deposit are composed of $CaCO_3$; validated in the XRD data (Fig. 3a, c). The surface morphology also depicts microcracks, which suggests possible swelling and subsequent shrinkage of carbon during the pyrolysis-activation.

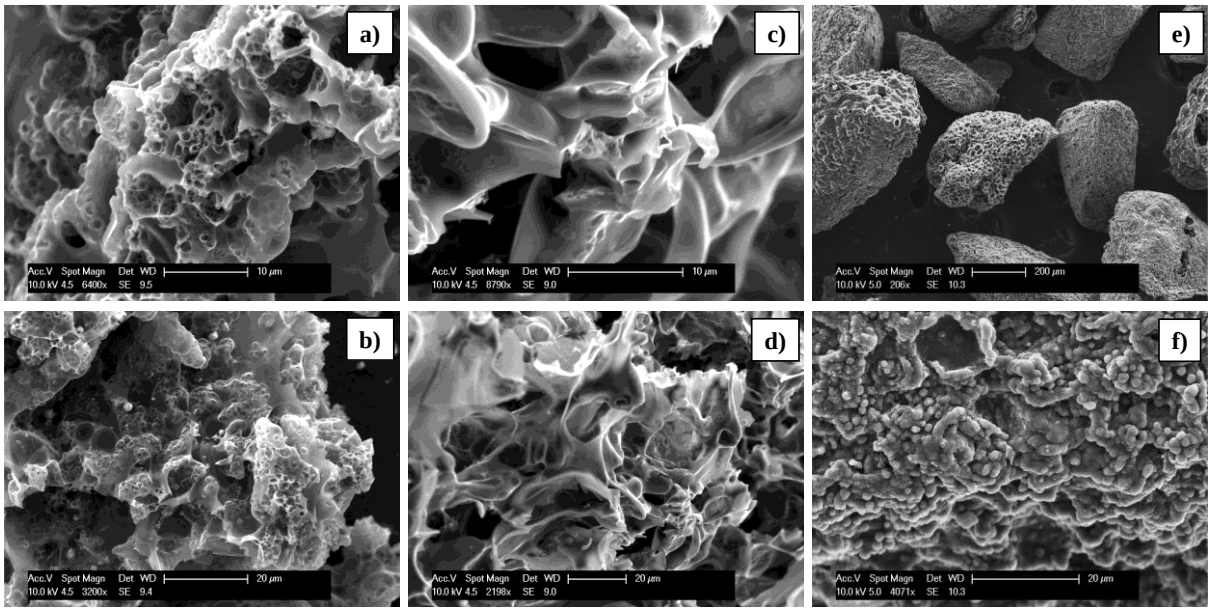

Fig. 4. SEM images of activated carbons prepared by direct pyrolysis-activation in microwave heating, 300-6-KOH (a,b) and 300-6-K_2CO_3 (c,d). PNS biochar 300-6 without chemical activation for comparison (e,f).

Thermogravimetric analysis (TGA) was used to characterise the thermal stability of the prepared activated carbons. As shown in Fig. S2, both activated carbons 300-6-KOH and 300-6-K_2CO_3 show an initial mass loss below 100 °C, due to removal of water, followed by a mass loss after 700 and 500 °C for 300-6-KOH and 300-6-K_2CO_3, respectively. According to the TGA curves, the activated carbon 300-6-KOH shows better thermal stability (as indicated by the carbon burn off maxima at 700 °C) compared to 300-6-K_2CO_3 with the burn off maxima at 500 °C. It appears that sample 300-6-KOH is more thermally stable and this may be related to the increase in level of graphitisation due to a better microwave absorption when KOH is the activating agent, as discussed in section 3.1 (dielectric properties).

3.3 CO_2 adsorption studies

3.3.1 Relevance of ultra-micropores for CO_2 uptake

The CO_2 uptake capacity of the activated carbons was investigated at 0 and 25 °C using volumetric and gravimetric analysis. The CO_2 uptake isotherms for all materials prepared via microwave pyrolysis-activation are shown in Fig. 5 and the samples with better CO_2 uptake performance are summarised in Table 3. The highest CO_2 uptake at 1.1 bar was 5.3 and 4.58 mmol g^{-1} for 300-6-KOH and 300-6-K_2CO_3 at 0 °C and 3.7 and 3.3 mmol g^{-1} for 300-6-KOH and 300-K_2CO_3 at 25 °C. The CO_2 uptake clearly indicates that it is not the total surface area, but the pore size that actually determined the CO_2 uptake. As evidenced by XRD, sample 300-6-KOH appears to have calcium carbonate. In order to explore its potential effect on CO_2 capture performance, an additional experiment was performed using the calcium of sample 300-6-KOH (obtained from the ash). The results are presented in Fig. S3 b), and reveal a CO_2

adsorption of 0.05 mmol/g. This suggests that the calcium on the sample proposes minimal contribution to the overall performance of sample 300-6-KOH (at 25 °C and 1 bar) and may clog some porosity. This confirms the results reported in literature, the micropores are in face, a main key parameter in the uptake of CO_2.

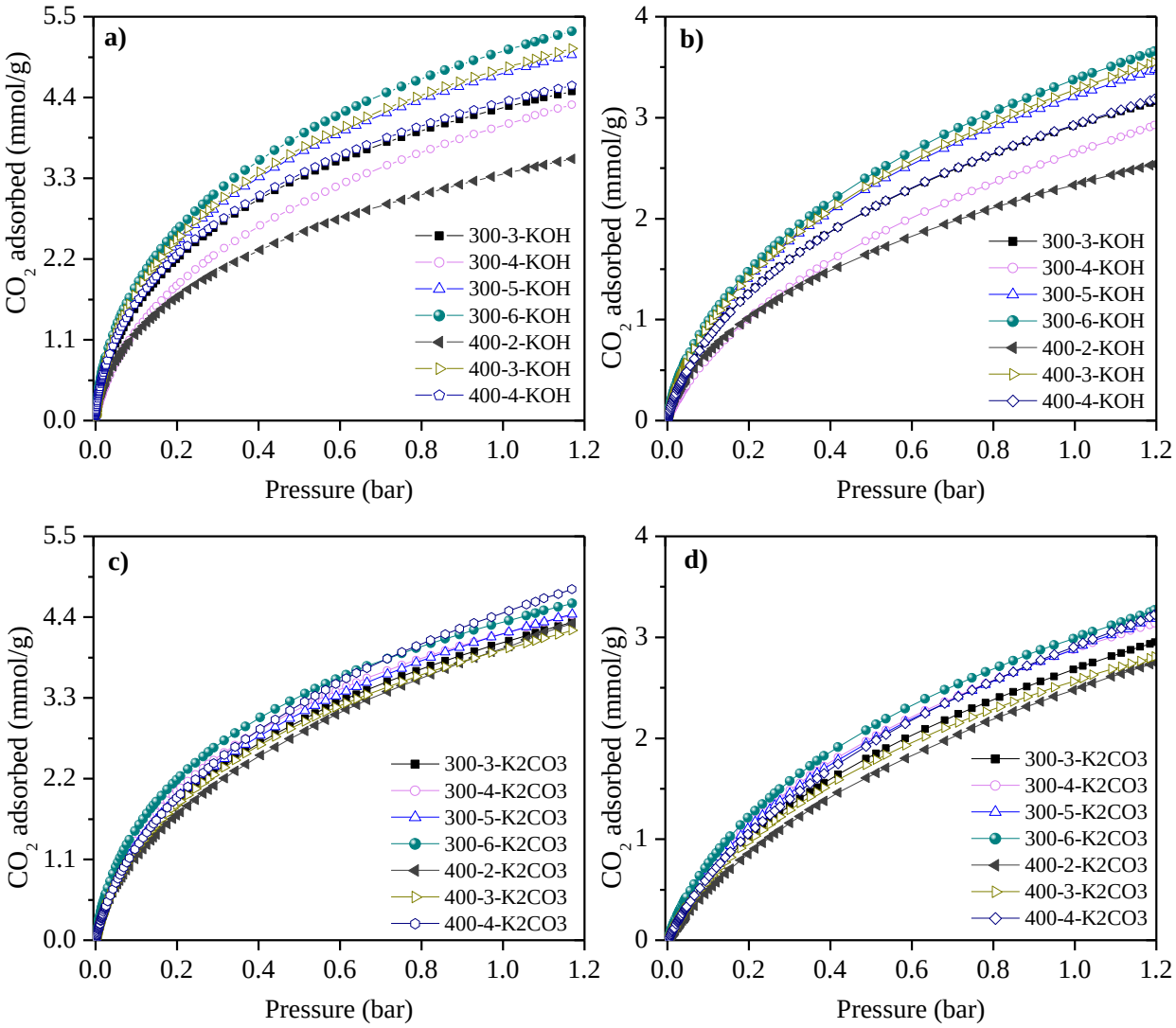

Fig. 5. CO_2 adsorption profiles at 0 °C and 25 °C for all KOH (a, b) and K_2CO_3 carbons (c, d) from the microwave pyrolysis-activation at different powers and times. Conditions: 100% CO_2

The surface area of 300-6-KOH and 300-6-K_2CO_3 carbons are 959 and 842 $m^2\ g^{-1}$, however 300-6-KOH possess 73.49% of ultra-micropores with a size of <0.8 nm, compared to 66.89%

in sample 300-6-K_2CO_3. Previously, it has been demonstrated that at pressures of 0-1 bar and temperatures of 0-25 °C, the enhancement of CO_2 uptake is negligible for micropores widths larger than around two to three times the molecular diameter (CO_2 diameter~0.33 nm) [16, 54]. This important finding is also in agreement with the results obtained in this study. To better understand the adsorption mechanism and reveal the significant effect of pore size, the fraction of ultra-micropore filling by CO_2 (f_{CO2}) was calculated [54] and is shown in Fig. 6. This parameter describes the relationship between the pore size and the pore filled by CO_2 and is defined as $f_{CO2}=q/(V_{<0.7nm}\cdot\rho_{CO2})$, where q is the CO_2 uptake, $V_{<0.7nm}$ is the ultra-micropore volume and ρ_{CO2} is the density of liquid CO_2 (1.03 g cm^{-3} at 0 ° C).

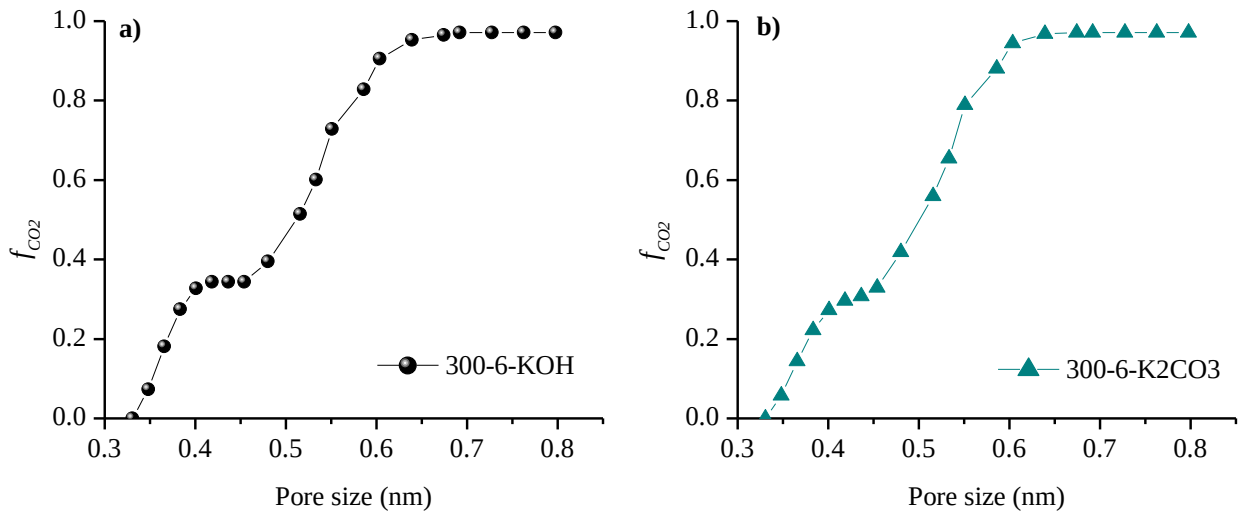

Fig. 6. Pore filled by CO_2 with average micropore size of sample 300-6-KOH (a) and 300-6-K_2CO_3 (b), deduced by applying the NLDFT model to CO_2 isotherms at 0 °C.

The results presented in Fig. 6 reveal that at pressures of 0-1 bar, the CO_2 adsorption is mainly determined by the ultra-micropores with a size below 0.8 nm. The results indicate the highest fraction of pore filled occurs in pores of size of 0.7 nm, whereas others pores such super-micropores (0.8-2 nm) are not relevant for CO_2 capture at this given conditions (0-1 bar). The results confirm that the adsorption mechanisms consist of volume-pore filling rather than

surface cover, which is typically observed in mesoporous materials. This validates the lack of a correlation between the CO_2 uptake and specific surface area (S_{BET}) and total pore volume (V_T); indicating that the interaction between adsorbents and CO_2 becomes stronger when the pore size decreases and the ideal pore size is around 0.7 nm. It is important to mention that the CO_2 adsorption at higher pressures (30-70 bar) could be enhanced by the super-micropores (0.8-2 nm) and as results of coverage adsorption mechanism [16].

It is worth to note that the CO_2 uptake of sample 300-6-KOH at 0 and 25 ° C (5.3 &3.7 mmol g^{-1}) is comparable or even higher to activated carbons with good performance for CO_2 uptake at 1.1 bar [45-47, 53, 55-57]. (See Table 3). Furthermore, all materials previously generated and tested for CO_2 uptake were prepared in two or three step processes that typically utilised a material that was already carbonised, which was then subsequently activated at a high impregnation ratio and temperature for longer processing times. Huang *et al*. [55] reported for first time the direct activation by microwaves of oil palm shell using an impregnation ratio of 2.5:1 of KOH:Oil palm shell and a microwave power of 750 W for 30 min. The maximum CO_2 uptake reported was 1.7 mmol g^{-1}, significantly lower than what was achieved herein. Also a comparable performance was achieved to the best templated activated carbons impregnated (KOH:hydrochar) with a ratio of 2:1 [49] and 6:1, [26] respectively. The CO_2 capture is only slightly exceeded by activated carbons derived from sawdust (4.9 mmol g^{-1}) [28] and examples of N-doped activated carbons (4.7-4.9 mmol g^{-1}) or composites [25, 58, 59]. However, it is important to highlight that the materials prepared in the present work have the advantage of a low impregnation ratio (1:1), which essentially circumvents a doping step. Furthermore, the short processing times represents a novel and energy-effective pathway for the development of such materials for a range of industrial applications.

Table 3. Comparative evaluation of CO_2 adsorption capacities and textural parameters of activated carbons prepared form different biomass.

Raw material	Carbonization (C) & Activation (A) (Temp. °C)/Residence time. min)	Agent	Agent:Biomass Agent:Char ratio	Microwave power/time (W/min)	CO_2 uptake at 1 bar (mmol g^{-1})/T (°C)	S_{BET} (m^2 g^{-1})	V_{tot} (cm^3 g^{-1})	V_{micro} (cm^3 g^{-1})	Ref.
*PNS	n/a	KOH	1:1	300/6	5.3/0	959	0.377	0.35	This work
*PNS	n/a	KOH	1:1	300/6	3.7/25	959	0.377	0.35	This work
*PNS	n/a	K_2CO_3	1:1	300/6	4.5 /0	974	0.401	0.35	This work
*PNS	n/a	K_2CO_3	1:1	300/6	3.3/25	974	0.401	0.35	This work
Oil palm shell	n/a	KOH	2.5:1	750/30	1.7/25	1069	0.52	0.42	[60]
Rice straw	-	-	-	200/20	1.75/25	122	0.08	0.03	[55]
Pitch	A-800/120	KOH	1:1	n/a	1.93/25	1012	0.422	0.374	[45]
Rice husk	A-600/60	KOH	1:1	n/a	3.25/25	536	0.24	0.19	[46]
Chestnut	C-600/120 A-800/120	NH_3	1.25:1	n/a	2.3/25	747	-	-	[47]
Corncob	C-800/180 A-800/180	NH_3-KOH	4:1	n/a	2.81/25	1154	0.57	-	[53]
Rice husk	C-900/60 A-100/60	K_2CO_3-CO_2	5:1	n/a	3.1/25	-	-	-	[56]
Empty fruit bunch	C-350/20 A-800/30	KOH	5:1	n/a	3.4/25	1322	0.78	0.23	[57]
Arundo donax	C+A-600/120	KOH	2:1	n/a	3.6/25	1122	0.59	0.50	[49]
Chitosan	A-600/60	K_2CO_3-NH_3	4:1	n/a	4.9/25	1355	0.60	0.47	[25]
Sawdust	C-250/120 A-600/60	KOH	2:1	n/a	4.9/25	1260	0.62	0.55	[28]
Black locust	C-650/180 A-800/90	KOH	6:1	n/a	3.75/25	2064	0.98	0.87	[26]
Pine cone	C-600/60 A-800/60	KOH-NH_3	3:1	n/a	4.7/25	1680	0.61	0.53	[58]

*Single step pyrolysis-activation

3.3.2 Adsorption kinetics and selectivity

An effective CO_2 carbon adsorbent should not only possess desirable characteristics such as a large surface area, high micropore volume and high CO_2 uptake capacity, but also have fast adsorption kinetics and suitability for use in swing cycles. The CO_2 adsorption kinetics for all materials and the selectivity of selected carbons against N_2 are shown in Fig. 7. The kinetics and selectivity curves for all materials were carried out in a thermogravimetric system at 25 °C, as described in section 2.5. It can be seen the rate of adsorption was exponential and the equilibrium uptake was achieved for samples 300-6-KOH and 300-6-K_2CO_3 in less than 3 min (Fig. 7a-b). This can be observed with detail in Fig. S4 and Fig. S5. It can be observed that the materials exhibit a short breakthrough time, in accordance with their equilibrium capacity, suggesting a low mass transfer resistance over the activated carbons. The low time required to reach the equilibrium, may be associated to the optimum pore size of the adsorbent which has been reported is two or three times the diameter of the adsorbate. Given the kinetic diameter of CO_2 is 0.33 nm, the optimum pore size is between 0.7 and 0.9 nm [43]. Therefore, the porosity and pore size in the activated carbons may play a crucial role in the CO_2 diffusion in the porous network. These results indicate that CO_2 can be separated effectively in short adsorption cycle times, which is of significant importance for practical industrial applications.

The selectivity of activated carbons was highlighted by comparing the CO_2 uptake with N_2 sorption at 25 °C and 1 bar for representative samples (300-6-KOH and 300-6-K_2CO_3). The CO_2 and N_2 uptake are compared in Fig. 7 (c-d). The CO_2 uptake for both samples is far higher than that of N_2, which only reached 0.09 mmol g^{-1} and 0.14 mmol g^{-1} for samples 300-6-KOH and 300-6-K_2CO_3, respectively. The α (CO_2/N_2) ratio measured at equilibrium conditions was 36.6 and 19.5 for both selected activated carbons. The selectivity of the materials prepared in this work was found to be very high and even higher than N-doped activated carbons (α (CO_2/N_2) = 6.5) [61, 62]. The results indicate the development of CO_2 selective adsorbents,

which are preferable and economically feasible since pure CO_2 can be extracted from the adsorbent and utilized as another carbon source for industry. The selectivity may depend on the different physical properties of the gas molecules such as polarizability or quadrupole moment. The results indicate the Van der Waals forces between N_2 molecules and the micropore carbon are weakerer than that of CO_2, which is expected due to the higher polarizability of CO_2 that has a greater affinity to carbon. In this sense the polarizability of CO_2 and N_2 is 29.1x10^{-25} cm^{-3} and 17.4 x10^{-25} cm^{-3} respectively, [57] and leads to achieve higher CO_2 selectivity.

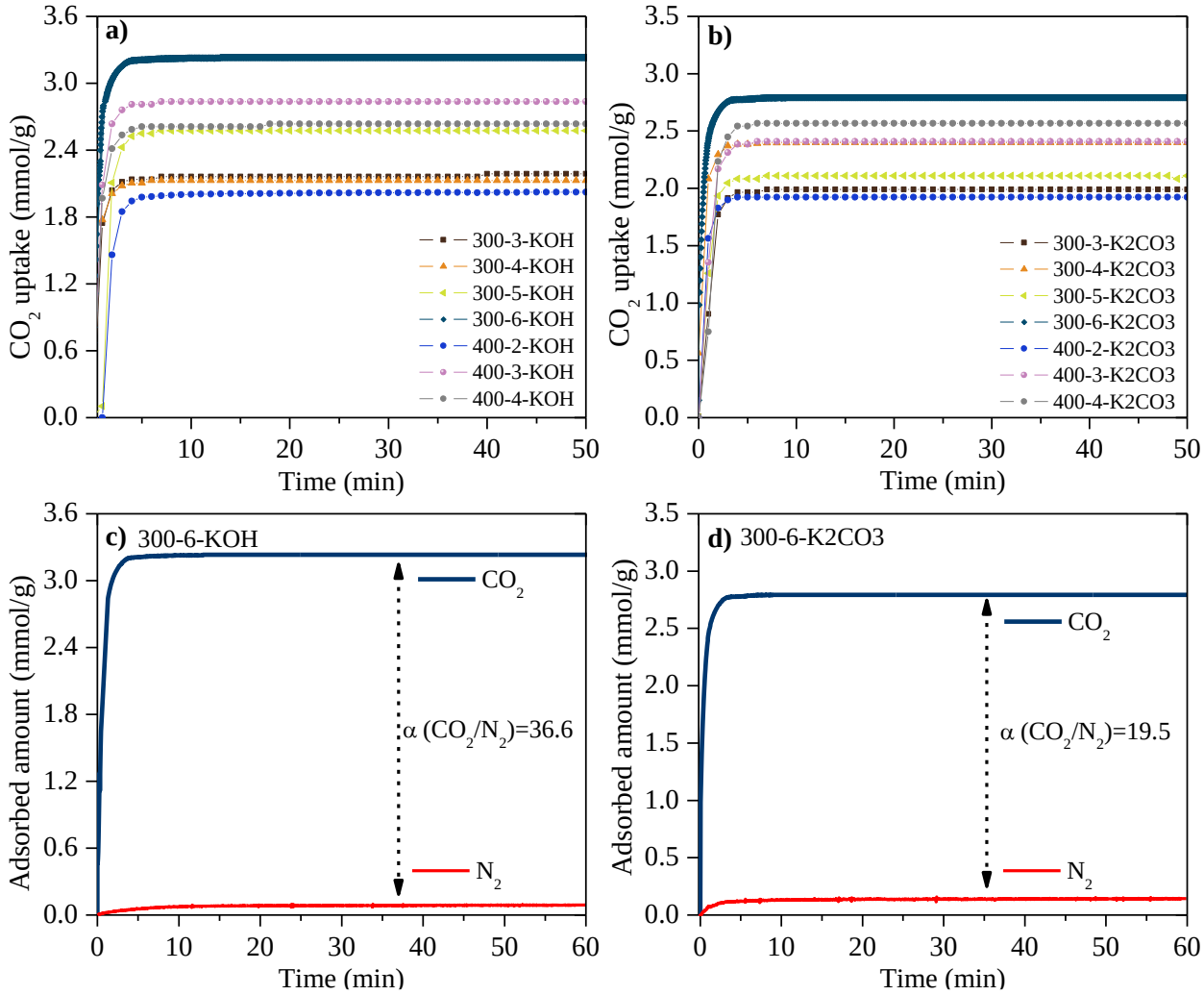

Fig. 7. Adsorption kinetics of CO_2 for all KOH (a) and K_2CO_3 (b) carbons from the microwave pyrolysis-activation at different conditions. Adsorption kinetics and selectivity of CO_2 and N_2 for sample 300-6-KOH (c) and 300-6-K_2CO_3 (d) Conditions: 1 bar, 25 °C.

3.3.3 High temperature CO_2 uptake

In order to evaluate the commercial application of the materials prepared in this work, the CO_2 capture uptake was explored at higher temperatures (25 – 100 °C) to simulate their performance in post-combustion capture. The results of 100% CO_2 and 15% CO_2 at 1 bar are shown in Fig. 8. As expected, the CO_2 uptake decreased at higher temperatures. At 40 °C and 100% CO_2 the sample 300-6-KOH absorbed 2.47 mmol g^{-1} and decreased to 0.62 mmol g^{-1} at 100 °C. This is because at higher temperature the CO_2 have a higher molecular kinetic energy, which allows CO_2 to escape form the adsorbent. In many industrial processes, the CO_2 is produced as flue gas at 15% CO_2 and 1 bar, at these conditions, the CO_2 uptake is more challenging and decreases from 0.94 to 0.22 mmol g^{-1} in the same range of temperature. The values are comparable to the values reported previously for hierarchical carbons [63]. The results indicate the adsorbents prepared in this work could be promising candidates for greater uptake at higher pressures.

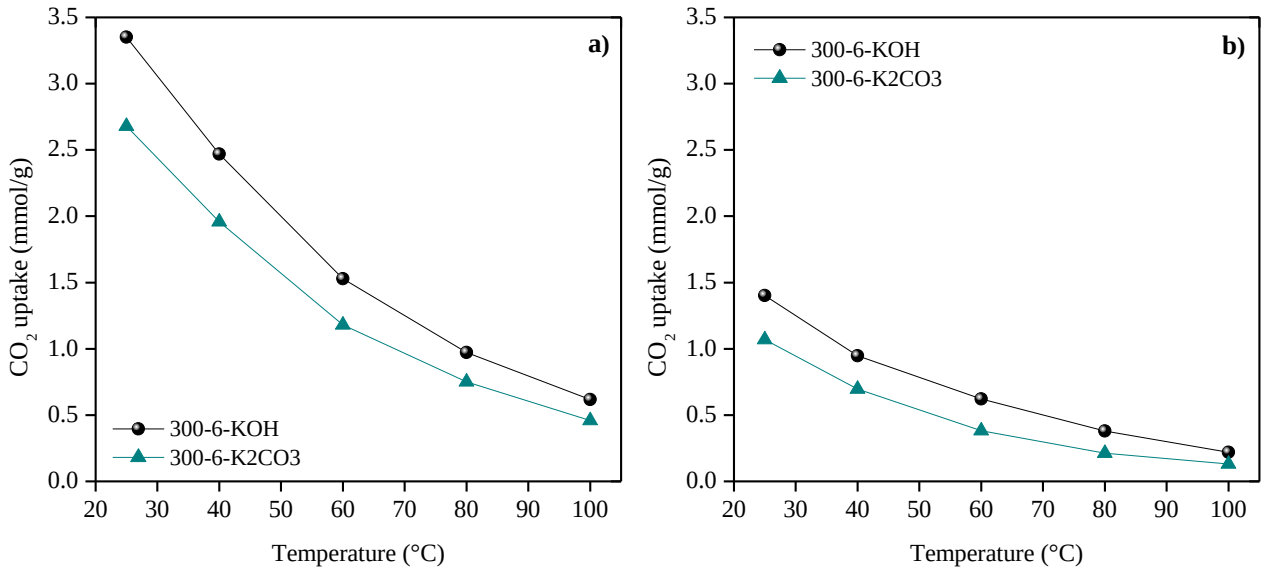

Fig. 8. CO_2 uptake of 300-6-KOH and 300-6-K_2CO_3 in a 100% (a) and 15% (vol% CO_2) gas flow at different temperatures

3.3.4 Isosteric heat

In order to investigate the interaction strength between the CO_2 and the adsorbents, the isosteric heats of adsorption (Q_{st}) were calculated via the CO_2 adsorption isotherms at 0 and 25 °C and by applying the Clausius-Clapeyron equation. The adsorption data at different temperatures (Fig. 9a) and the relationship between the values of Q_{st} and CO_2 adsorption capacities are plotted in Fig. 9 (Fig. 9b). At the initial stage, 300-6-KOH exhibits a high Q_{st} of 37.4 kJ mol^{-1} and at a steady stage of 28.2 kJ mol^{-1}, which is even higher than previously reported values of porous carbons (e.g. 20.3-27.7 kJ mol^{-1}, [64] 21.3–24.2 kJ mol^{-1}, [65] 35.9-21.1 kJ mol^{-1}, [66]). Sample 300-6-K_2CO_3 exhibited a lower Q_{st} of 34.2-25.0 kJ mol^{-1}. The higher Q_{st} value of 300-6-KOH in the initial adsorption stage is an indicator of the strong gas molecules interaction with the network of porous carbon, which can be explained by the quadrupolar interaction between CO_2 molecules and ultra-micropores with narrow pore size distribution (0.7 nm) [66]. At lower CO_2 uptake, the Q_{st} value of both samples are greater than the values reported for chemi-sorption (greater than 30 kJ mol^{-1}) [67], however at higher CO_2 uptakes, the Q_{st} values are much smaller, indicating CO_2 adsorption involves mechanisms of physical adsorption and suggesting a reversible process that implies low energy in the regeneration process.

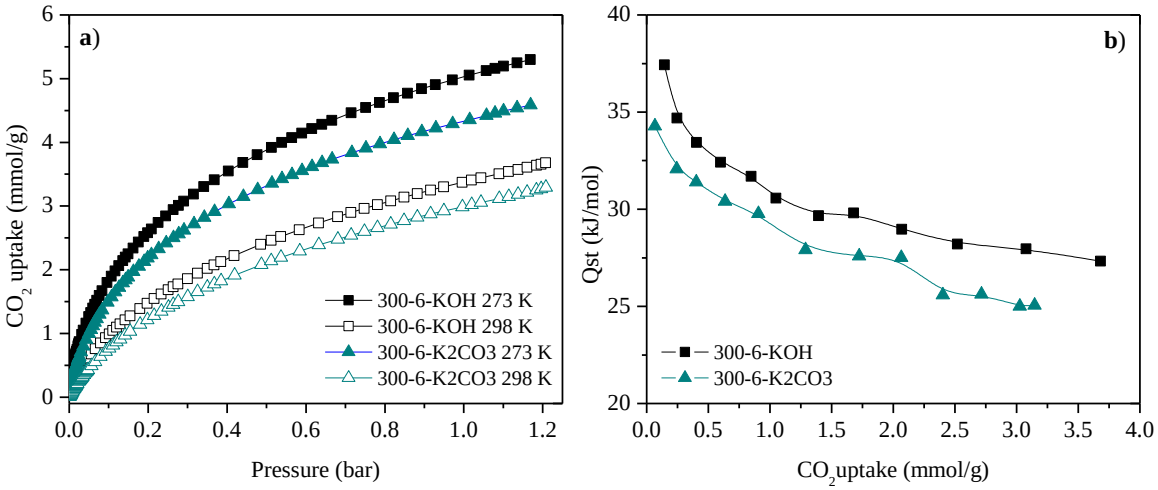

Fig. 9. CO_2 adsorption isotherms of 300-6-KOH and 300-6-K_2CO_3 samples at 1 bar and 0 and 25 °C (a); Isosteric heat of CO_2 adsorption for 300-6-KOH and 300-6-K_2CO_3 at different CO_2 uptakes (b).

The high Q_{st} value and the narrow micropores of sample 300-6-KOH (See Fig. 9b) predict stronger interactions between the carbon and CO_2 molecules. Indeed the results emphasise the importance of the pore size and surface, nevertheless 300-6-K_2CO_3 possesses higher surface area and has lower Q_{st} compared to 300-6-KOH. Thus the ultra-micropores and high Q_{st} of 300-6-KOH emphasise the synergetic effects of textural parameters leading to superior CO_2 uptake. The high Q_{st} is ascribed to the optimal (with respect to CO_2 adsorption) pore size. It is envisaged that narrow micropores engender stronger interactions between adsorbents and CO_2 molecules than larger micropores or mesopores. Indeed, the importance of pore size is emphasised by the fact that sample 300-6-KOH possesses higher volume of ultra-micropores compared with 300-6-K_2CO_3, evidenced in Table 2 and Fig. 2.

It is important to highlight the materials prepared in the present work, were prepared using a waste precursor (PNS) using a low concentration of chemical agent, in a single step of pyrolysis-activation and in a very short time (6 min), allowing an easy, green and sustainable synthesis.

3.3.5 Adsorbents reuse and CO_2 adsorption cycles

Besides attaining a high uptake capacity and fast adsorption kinetics, an effective adsorbent that can be used within CO_2 capture systems must also exhibit high reusability properties, as this highlights the efficiency and economics of the CO_2 capture process. In this sense, the adsorption/desorption cycles of samples 300-6-KOH and 300-6-K_2CO_3 at 100 and 15% CO_2 are shown in Fig. 10. The experiments were conducted at adsorption (CO_2)-desorption (N_2) pressure of 1 bar and 25 °C. The results showed that the CO_2 adsorbed can be easily desorbed after the carrier gas is switched from CO_2 to N_2. These results indicate that after several adsorption-desorption cycles, the activated carbons maintain their adsorption capacity. Specifically the adsorption efficiency was maintained at 97-100% after the 20^{th} cycle, which demonstrates high chemical and physical stability. Thus, CO_2 capture in both activated carbons is highly reversible and primarily based on physi-sorption. The simple and straight forward regeneration of 300-6-KOH and 300-6-K_2CO_3 make them superior adsorbents compared to aqueous amine-adsorbents, which require large amounts of energy during the regeneration process [7]. This enables this technology to deliver high viability for scale-up and easy fabrication.

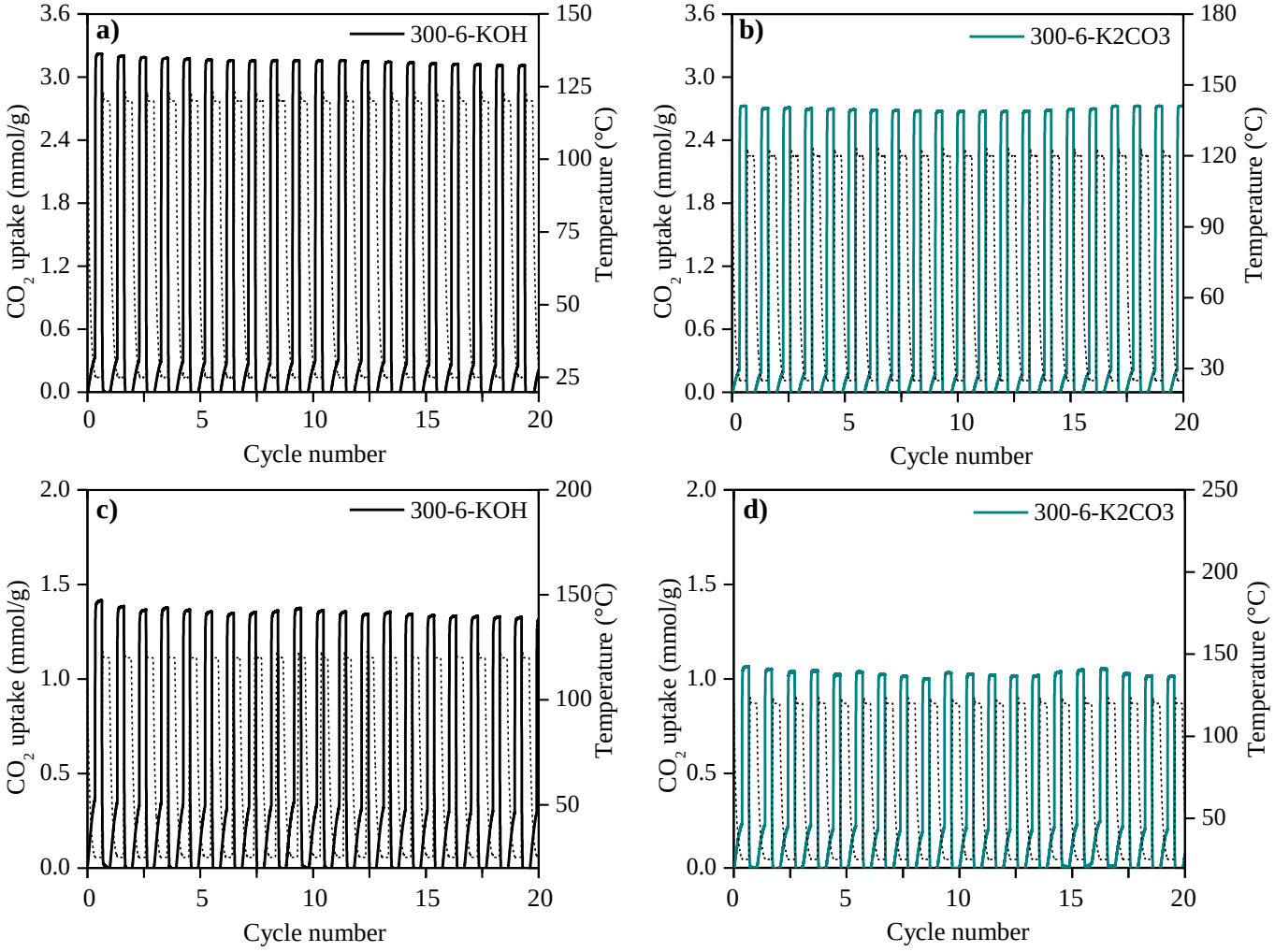

Fig. 10. CO_2 uptake of 300-6-KOH and 300-6-K_2CO_3 (b, d) in a 100 % vol (a, b) and 15% vol (c, d) CO_2 gas flow at 25 °C in 20 five cycles of adsorption and desorption.

4 Conclusions

In summary, the work described herein has shown that a sustainable and a simple microwave thermal treatment can be implemented to prepare ultra-microporous activated carbons from a biomass waste feedstock in a direct pyrolysis-activation step by using low KOH and K_2CO_3 impregnation ratio of 1. A rapid and simple route to synthesizing porous materials with high CO_2 uptake and selectivity has been established. The highest CO_2 uptake is 5.3 mmol g^{-1} at 1 bar and 0 °C, which is one of the largest reported in literature for porous carbons using low agent ratio. Depending on the microwave heating conditions, the activated carbons have from a modest to high surface areas ranging from 600 to 1000 m^2 g^{-1}, of which up to 73% of the surface area arises from ultra-micropores (<0.8nm). The CO_2 uptake capacity for the activated carbons is due to the narrow micropores (~0.7 nm), enhancing its selectivity and simple regeneration after 20 cycles and in short adsorption cycle times, which is of significant importance for practical industrial applications. The present results suggest that an effective and green route with considerable energy savings can be implemented to prepare activated carbon porous materials for CO_2 uptake and may be favourable for parallel applications such as liquid adsorption, catalysis and energy storage.

Conflicts of interest

There are no conflicts to declare.

Acknowledgements

This research was supported by the Council of Science and Technology (CONACyT), Mexico under the grant 389535.

References

1. Estevez, L., et al., *Hierarchically Porous Carbon Materials for CO2 Capture: The Role of Pore Structure.* Industrial & Engineering Chemistry Research, 2018. **57**(4): p. 1262-1268.
2. D'Alessandro, D.M., B. Smit, and J.R. Long, *Carbon dioxide capture: prospects for new materials.* Angewandte Chemie International Edition, 2010. **49**(35): p. 6058-6082.
3. Sethia, G. and A. Sayari, *Nitrogen-doped carbons: remarkably stable materials for CO2 capture.* Energy & Fuels, 2014. **28**(4): p. 2727-2731.
4. Singh, G., et al., *Biomass derived porous carbon for CO2 capture.* Carbon, 2019.
5. Nations, U. *Climate action*. 27/01/2020]; Available from: https://www.un.org/en/climatechange/index.shtml.
6. Nations, U. *Paris Agreement to the United Nations Framework Convention on Climate Change*. 2015 27/01/2020]; Available from: https://unfccc.int/process-and-meetings/the-paris-agreement/the-paris-agreement.
7. Rashidi, N.A. and S. Yusup, *An overview of activated carbons utilization for the post-combustion carbon dioxide capture.* Journal of CO2 Utilization, 2016. **13**: p. 1-16.
8. Gholidoust, A., J.D. Atkinson, and Z. Hashisho, *Enhancing CO2 adsorption via amine-impregnated activated carbon from oil sands coke.* Energy & Fuels, 2017. **31**(2): p. 1756-1763.
9. Hasib-ur-Rahman, M., M. Siaj, and F. Larachi, *CO2 capture in alkanolamine/room-temperature ionic liquid emulsions: A viable approach with carbamate crystallization and curbed corrosion behavior.* International Journal of Greenhouse Gas Control, 2012. **6**: p. 246-252.
10. Veneman, R., H. Kamphuis, and D.W.F. Brilman, *Post-Combustion CO2 capture using supported amine sorbents: A process integration study.* Energy Procedia, 2013. **37**: p. 2100-2108.
11. Samanta, A., et al., *Post-combustion CO2 capture using solid sorbents: a review.* Industrial & Engineering Chemistry Research, 2011. **51**(4): p. 1438-1463.
12. Olivares-Marín, M. and M.M. Maroto-Valer, *Development of adsorbents for CO2 capture from waste materials: a review.* Greenhouse Gases: Science and Technology, 2012. **2**(1): p. 20-35.
13. Zhang, H., et al., *Green and rapid synthesis of hierarchical porous zeolitic imidazolate frameworks for enhanced CO2 capture.* Inorganica Chimica Acta, 2018. **482**: p. 358-363.
14. Jiang, Y., et al., *Simultaneous biogas purification and CO2 capture by vacuum swing adsorption using zeolite NaUSY.* Chemical Engineering Journal, 2018. **334**: p. 2593-2602.
15. Alabadi, A., et al., *Highly porous activated carbon materials from carbonized biomass with high CO2 capturing capacity.* Chemical Engineering Journal, 2015. **281**: p. 606-612.
16. Zhang, Z., et al., *In-situ ion-activated carbon nanospheres with tunable ultramicroporosity for superior CO2 capture.* Carbon, 2019. **143**: p. 531-541.
17. Liu, W., et al., *Performance enhancement of calcium oxide sorbents for cyclic CO2 capture – A review.* Energy & Fuels, 2012. **26**(5): p. 2751-2767.
18. Song, G., et al., *An investigation of CO2 adsorption kinetics on porous magnesium oxide.* Chemical Engineering Journal, 2016. **283**: p. 175-183.
19. Hu, Z., et al., *Ionized Zr-MOFs for highly efficient post-combustion CO2 capture.* Chemical Engineering Science, 2015. **124**: p. 61-69.
20. Gray, M., et al., *CO2 capture by amine-enriched fly ash carbon sorbents.* Separation and Purification Technology, 2004. **35**(1): p. 31-36.
21. Li, D., et al., *Influence of doping nitrogen, sulfur, and phosphorus on activated carbons for gas adsorption of H 2, CH 4 and CO 2.* RSC Advances, 2016. **6**(55): p. 50138-50143.

22. Sangchoom, W. and R. Mokaya, *Valorization of lignin waste: carbons from hydrothermal carbonization of renewable lignin as superior sorbents for CO2 and hydrogen storage.* ACS Sustainable Chemistry & Engineering, 2015. **3**(7): p. 1658-1667.
23. Liew, R.K., et al., *Microwave pyrolysis with KOH/NaOH mixture activation: A new approach to produce micro-mesoporous activated carbon for textile dye adsorption.* Bioresource technology, 2018. **266**: p. 1-10.
24. Wickramaratne, N.P., et al., *Nitrogen enriched porous carbon spheres: attractive materials for supercapacitor electrodes and CO2 adsorption.* Chemistry of Materials, 2014. **26**(9): p. 2820-2828.
25. Fujiki, J. and K. Yogo, *The increased CO 2 adsorption performance of chitosan-derived activated carbons with nitrogen-doping.* Chemical Communications, 2016. **52**(1): p. 186-189.
26. Zhang, C., et al., *Enhancement of CO2 capture on biomass-based carbon from black locust by KOH activation and ammonia modification.* Energy & Fuels, 2016. **30**(5): p. 4181-4190.
27. Lakhi, K.S., et al., *Energy efficient synthesis of highly ordered mesoporous carbon nitrides with uniform rods and their superior CO 2 adsorption capacity.* Journal of Materials Chemistry A, 2017. **5**(31): p. 16220-16230.
28. Sevilla, M. and A.B. Fuertes, *Sustainable porous carbons with a superior performance for CO 2 capture.* Energy & Environmental Science, 2011. **4**(5): p. 1765-1771.
29. Tan, I., et al., *Adsorption behavior of cadmium ions onto phosphoric acid-impregnated microwave-induced mesoporous activated carbon.* Journal of Water Process Engineering, 2016. **14**: p. 60-70.
30. Kostas, E.T., D. Beneroso, and J.P. Robinson, *The application of microwave heating in bioenergy: A review on the microwave pre-treatment and upgrading technologies for biomass.* Renewable and Sustainable Energy Reviews, 2017. **77**: p. 12-27.
31. Georgin, J., et al., *Preparation of activated carbon from peanut shell by conventional pyrolysis and microwave irradiation-pyrolysis to remove organic dyes from aqueous solutions.* Journal of Environmental Chemical Engineering, 2016. **4**(1): p. 266-275.
32. Jimenez, G.D., et al., *New insights into microwave pyrolysis of biomass: Preparation of carbon-based products from pecan nutshells and their application in wastewater treatment.* Journal of Analytical and Applied Pyrolysis, 2017.
33. Jimenez, G.D., et al., *New insights into microwave pyrolysis of biomass: Preparation of carbon-based products from pecan nutshells and their application in wastewater treatment.* Journal of Analytical and Applied Pyrolysis, 2017. **124**: p. 113-121.
34. Metaxas, A.C. and R.J. Meredith, *Industrial Microwave Heating*. 1983, London, U.K.: Peter Peregrinus Ltd.
35. Motasemi, F., et al., *Microwave dielectric characterization of switchgrass for bioenergy and biofuel.* Fuel, 2014. **124**: p. 151-157.
36. Kabir, M.F., et al., *Temperature dependence of the dielectric properties of rubber wood.* Wood and Fiber science, 2007. **33**(2): p. 233-238.
37. Motasemi, F., A.A. Salema, and M.T. Afzal, *Dielectric characterization of corn stover for microwave processing technology.* Fuel Processing Technology, 2015. **131**: p. 370-375.
38. Tripathi, M., et al., *Effect of temperature on dielectric properties and penetration depth of oil palm shell (OPS) and OPS char synthesized by microwave pyrolysis of OPS.* Fuel, 2015. **153**: p. 257-266.
39. Ramasamy, S. and B. Moghtaderi, *Dielectric properties of typical Australian wood-based biomass materials at microwave frequency.* Energy & Fuels, 2010. **24**(8): p. 4534-4548.
40. Omar, R., et al., *Characterization of empty fruit bunch for microwave-assisted pyrolysis.* Fuel, 2011. **90**(4): p. 1536-1544.
41. Menéndez, J., et al., *Microwave heating processes involving carbon materials.* Fuel Processing Technology, 2010. **91**(1): p. 1-8.

42. Beneroso, D., et al., *Dielectric characterization of biodegradable wastes during pyrolysis.* Fuel, 2016. **172**: p. 146-152.
43. Coromina, H.M., D.A. Walsh, and R. Mokaya, *Biomass-derived activated carbon with simultaneously enhanced CO 2 uptake for both pre and post combustion capture applications.* Journal of Materials Chemistry A, 2016. **4**(1): p. 280-289.
44. Thommes, M., et al., *Physisorption of gases, with special reference to the evaluation of surface area and pore size distribution (IUPAC Technical Report).* Pure and Applied Chemistry, 2015. **87**(9-10): p. 1051-1069.
45. Lee, S.-Y., et al., *Preparation and characterization of pitch-based nanoporous carbons for improving CO2 capture.* Journal of Solid State Chemistry, 2014. **215**: p. 201-205.
46. Liu, X., et al., *Potassium and zeolitic structure modified ultra-microporous adsorbent materials from a renewable feedstock with favorable surface chemistry for CO2 capture.* ACS applied materials & interfaces, 2017. **9**(32): p. 26826-26839.
47. Nelson, K.M., et al., *Preparation and CO2 adsorption properties of soft-templated mesoporous carbons derived from chestnut tannin precursors.* Microporous and Mesoporous Materials, 2016. **222**: p. 94-103.
48. Zhu, S., et al., *Soluble salt self-assembly-assisted synthesis of three-dimensional hierarchical porous carbon networks for supercapacitors.* Journal of Materials Chemistry A, 2015. **3**(44): p. 22266-22273.
49. Singh, G., et al., *Single step synthesis of activated bio-carbons with a high surface area and their excellent CO2 adsorption capacity.* Carbon, 2017. **116**: p. 448-455.
50. El-Hendawy, A.-N.A., *An insight into the KOH activation mechanism through the production of microporous activated carbon for the removal of Pb2+ cations.* Applied Surface Science, 2009. **255**(6): p. 3723-3730.
51. Wang, J. and S. Kaskel, *KOH activation of carbon-based materials for energy storage.* Journal of Materials Chemistry, 2012. **22**(45): p. 23710-23725.
52. Adeniran, B., E. Masika, and R. Mokaya, *A family of microporous carbons prepared via a simple metal salt carbonization route with high selectivity for exceptional gravimetric and volumetric post-combustion CO 2 capture.* Journal of Materials Chemistry A, 2014. **2**(35): p. 14696-14710.
53. Geng, Z., et al., *One-step synthesis of microporous carbon monoliths derived from biomass with high nitrogen doping content for highly selective CO 2 capture.* Scientific reports, 2016. **6**: p. 30049.
54. Sevilla, M., J.B. Parra, and A.B. Fuertes, *Assessment of the role of micropore size and N-doping in CO2 capture by porous carbons.* ACS applied materials & interfaces, 2013. **5**(13): p. 6360-6368.
55. Huang, Y.-F., et al., *Microwave pyrolysis of rice straw to produce biochar as an adsorbent for CO2 capture.* Energy, 2015. **84**: p. 75-82.
56. Li, M. and R. Xiao, *Preparation of a dual pore structure activated carbon from rice husk char as an adsorbent for CO2 capture.* Fuel Processing Technology, 2019. **186**: p. 35-39.
57. Parshetti, G.K., S. Chowdhury, and R. Balasubramanian, *Biomass derived low-cost microporous adsorbents for efficient CO2 capture.* Fuel, 2015. **148**: p. 246-254.
58. Zhu, B., C. Shang, and Z. Guo, *Naturally nitrogen and calcium-doped nanoporous carbon from pine cone with superior CO2 capture capacities.* ACS Sustainable Chemistry & Engineering, 2016. **4**(3): p. 1050-1057.
59. Kayal, S. and A. Chakraborty, *Activated carbon (type Maxsorb-III) and MIL-101 (Cr) metal organic framework based composite adsorbent for higher CH4 storage and CO2 capture.* Chemical Engineering Journal, 2018. **334**: p. 780-788.
60. Hesas, R.H., et al., *Microwave-assisted production of activated carbons from oil palm shell in the presence of CO2 or N2 for CO2 adsorption.* Journal of Industrial and Engineering Chemistry, 2015. **24**: p. 196-205.

61. Wei, H., et al., *Granular bamboo-derived activated carbon for high CO2 adsorption: the dominant role of narrow micropores.* ChemSusChem, 2012. **5**(12): p. 2354-2360.
62. Sevilla, M. and A.B. Fuertes, *CO2 adsorption by activated templated carbons.* Journal of colloid and interface science, 2012. **366**(1): p. 147-154.
63. Srinivas, G., et al., *Exceptional CO 2 capture in a hierarchically porous carbon with simultaneous high surface area and pore volume.* Energy & Environmental Science, 2014. **7**(1): p. 335-342.
64. Wickramaratne, N.P. and M. Jaroniec, *Activated carbon spheres for CO2 adsorption.* ACS applied materials & interfaces, 2013. **5**(5): p. 1849-1855.
65. Hong, S.-M., et al., *Porous carbon based on polyvinylidene fluoride: Enhancement of CO2 adsorption by physical activation.* Carbon, 2016. **99**: p. 354-360.
66. Hao, G.-P., et al., *Structurally designed synthesis of mechanically stable poly (benzoxazine-co-resol)-based porous carbon monoliths and their application as high-performance CO2 capture sorbents.* Journal of the American Chemical Society, 2011. **133**(29): p. 11378-11388.
67. Wei, Y., et al., *Periodic mesoporous organosilica nanocubes with ultrahigh surface areas for efficient CO 2 adsorption.* Scientific reports, 2016. **6**: p. 20769.